Molecular Therapy
Oncolytics
Original Article

LukS-PV Inhibits Hepatocellular Carcinoma Progression by Downregulating HDAC2 Expression

Ziran Wang,[1,5] Wenwei Yu,[2,5] Yawen Qiang,[1,5] Liangfei Xu,[1] Fan Ma,[1] Pengsheng Ding,[3] Lan Shi,[3] Wenjiao Chang,[3] Yide Mei,[4] and Xiaoling Ma[3]

[1]Department of Clinical Laboratory, Affiliated Provincial Hospital of Anhui Medical University, Hefei, Anhui, China; [2]Center of Reproductive Medicine, The First Affiliated Hospital of Anhui Medical University, Hefei, Anhui, China; [3]Department of Clinical Laboratory, The First Affiliated Hospital of USTC, Division of Life Sciences and Medicine, University of Science and Technology of China, Hefei, Anhui, China; [4]Division of Molecular Medicine, Hefei National Laboratory for Physical Sciences at Microscale, First Affiliated Hospital of University of Science and Technology of China, School of Life Sciences, University of Science and Technology of China, Hefei, Anhui, China

Hepatocellular carcinoma (HCC) is a common malignant tumor. LukS-PV is the S component of Panton-Valetine leukocidin (PVL), which is secreted by *Staphylococcus aureus*. This study investigated the effects of LukS-PV on the proliferation, apoptosis, and cell-cycle progression of HCC cells and the mechanisms of its activity. The HCC cells were treated with different LukS-PV concentrations *in vitro*. Cell Counting Kit-8 and 5-Ethynyl-2'-deoxyuridine (EdU) assays were used to study cell proliferation. Flow cytometry was used to measure apoptosis and cell-cycle progression. Quantitative reverse transcriptase PCR and western blot assays were used to determine mRNA and protein expression levels. Xenograft experiments were performed to determine the *in vivo* antitumor effect of LukS-PV. Immunostaining was performed to analyze Ki-67 and HDAC2 (histone deacetylase 2) expression. Our results showed that LukS-PV inhibited cell proliferation and induced apoptosis in a concentration-dependent manner in HCC cell lines. LukS-PV also can induce cell-cycle arrest. Moreover, we discovered that LukS-PV attenuated HDAC2 expression and upregulated PTEN; phosphorylated AKT was also reduced. Further studies demonstrated that LukS-PV treatment significantly reduced tumor growth in nude mice and suppressed Ki-67 and HDAC2 levels. Our data revealed a vital role of LukS-PV in suppressing HCC progression by downregulating HDAC2 and upregulating PTEN.

INTRODUCTION

Liver cancer is the sixth most common tumor worldwide and has extremely high morbidity and mortality.[1] The current treatment for hepatocellular carcinoma (HCC) is surgical resection, but the postoperative 5-year survival rate following surgery is only 10%,[2] highlighting the need for new treatment options.

The specificity and cytotoxicity of bacterial toxins for target cells have become a hotspot for the development of new antitumor drugs, and some bacterial toxins have been clinically used, such as botulinum neurotoxin type A, which is produced by strains of *Clostridium botulinum* and exhibits anticancer activity in prostate and breast cancer.[3] Diphtheria toxin from *Corynebacterium diphtheriae* exhibits anticancer activity in various preclinical models, including adrenocortical carcinoma, glioblastoma, cutaneous T cell lymphoma, breast carcinoma, and cervical adenocarcinoma.[4,5] Exotoxin A secreted by *Pseudomonas aeruginosa* has anticancer activity in pancreatic cancer, melanoma, head and neck squamous carcinoma, Burkitt's lymphoma, and leukemia.[6–8] Listeriolysin produced by strains of *Listeria monocytogenes* exhibits anticancer activity in breast carcinoma and leukemia.[9–11] LukS-PV (S component of Panton-Valetine leukocidin [PVL]) is a leukocidal cytotoxin secreted by *Staphylococcus aureus*, and our previous studies showed that it can inhibit leukemia cell proliferation and induce apoptosis.[12] *In vivo* studies have shown that LukS-PV has no obvious side effects.[13] Further research found that LukS-PV exerted antitumor effects through the C5a receptor (C5aR).[14]

C5aR is a receptor for complement C5a, and recently it was found to be highly expressed in a variety of tumors.[15–19] Hu et al.[16] found that C5aR was highly expressed in liver cancer, but negligibly expressed in adjacent tissues. Following our discovery that LukS-PV exerted antitumor effects through C5aR,[14] we hypothesized that it might also have antitumor effects in HCC cells that highly express C5aR.

Histone acetylation is dynamically regulated by histone acetyltransferases (HATs) and histone deacetylases (HDACs). HATs result in relaxation of chromatin structure and transcriptional activation of genes, while HDACs lead to chromatin condensation and are involved in transcriptional silencing.[20] Recent studies have suggested a correlation between histone acetylation or deacetylation and the development and progression of tumors.[21,22] HDACs are

Received 7 May 2020; accepted 20 May 2020;
https://doi.org/10.1016/j.omto.2020.05.006.

[5]These authors contributed equally to this work.

Correspondence: Xiaoling Ma, Department of Clinical Laboratory, The First Affiliated Hospital of USTC, Division of Life Sciences and Medicine, University of Science and Technology of China, No. 17 Lujiang Road, Hefei, Anhui 230001, China.
E-mail: maxiaoling@ustc.edu.cn

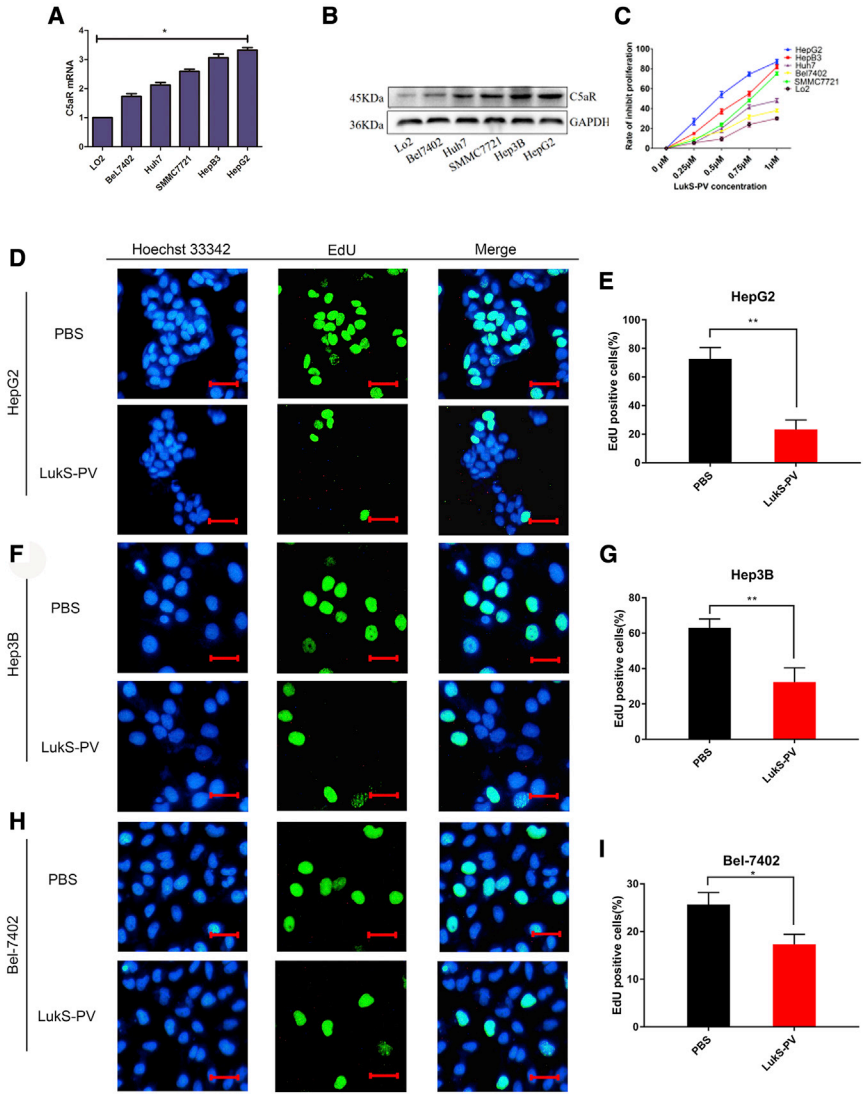

Figure 1. LukS-PV Inhibited the Proliferation of HCC Cells that Express C5aR

(A) qRT-PCR was applied to detect endogenous mRNA levels of C5aR in L02 and HCC cells. (B) Western blot was applied to detect endogenous protein levels of C5aR in L02 and HCC cells. (C) The rate of inhibiting proliferation was calculated in HCC cells treated with different concentrations of LukS-PV for 24 h. (D) EdU assays were conducted to detect the impact of LukS-PV on proliferation in HepG2 cells. (E) EdU positive cells were calculated in HepG2 cells. (F) EdU assays were conducted to detect the impact of LukS-PV on proliferation in Hep3B cells. (G) EdU positive cells were calculated in Hep3B cells. (H) EdU assays were conducted to detect the impact of LukS-PV on proliferation in Bel-7402 cells. (I) EdU positive cells were calculated in Bel-7402 cells. Scale bars, 20 μm.

overexpressed in different tumors types, and HDAC expression levels are closely related to prognosis.[23–25] Inhibition of HDACs can induce cell growth arrest and apoptosis in a variety of malignant cells, including breast cancer cells,[26] prostate cancer cells,[27] HCC cells,[28] pancreatic cancer cells,[29] lymphoma cells,[30] and lung cancer cells.[31] Thus, HDACs are considered therapeutic targets for various tumors.

In this study, we investigated the effects of LukS-PV on the proliferation and apoptosis of HCC cells and further explored its molecular mechanism of action.

RESULTS

LukS-PV Inhibited the Proliferation of HCC Cells that Express C5aR

Our previous study showed that LukS-PV induces apoptosis in acute myeloid leukemia cells mediated by C5aR.[14] It has been reported that C5aR is overexpressed in HCC and plays an important role in HCC progression.[16] To investigate whether LukS-PV also inhibits the progression of HCC, we first examined C5aR expression in HCC cell lines and the normal hepatocyte cell line L02. Quantitative reverse transcriptase PCR (qRT-PCR) and western blot results showed that C5aR expression was significantly increased in HCC cells (Figures 1A and 1B). Next, we treated cells with different concentrations of LukS-PV for 24 h. The results showed that LukS-PV inhibited the proliferation of HCC cells in a concentration-dependent manner (Figure 1C). Furthermore, the inhibition rate was positively correlated with C5aR expression. Additionally, the EdU assay was used to further evaluate the effect of LukS-PV on the proliferation of HCC cells. As shown in Figures 1D–1I, the number of EdU-positive cells in the LukS-PV group was decreased compared with the control group. Therefore, we confirmed that LukS-PV inhibited the proliferation of HCC cells.

LukS-PV Induced Apoptosis in HCC Cells that Express C5aR

To study the effect on apoptosis, we treated HCC cells with different concentrations of LukS-PV for 24 h. The results showed that LukS-PV induced apoptosis in five HCC cell lines in a concentration-dependent manner (Figure 2A). Likewise, the rate of apoptosis was correlated with C5aR expression. To further investigate the molecular mechanism, we examined mitochondrial apoptosis-associated proteins in HCC cells. The results showed that LukS-PV increased Bax expression and decreased Bcl-2 expression, suggesting LukS-PV induced apoptosis through the mitochondrial pathway (Figures 2B–2D).

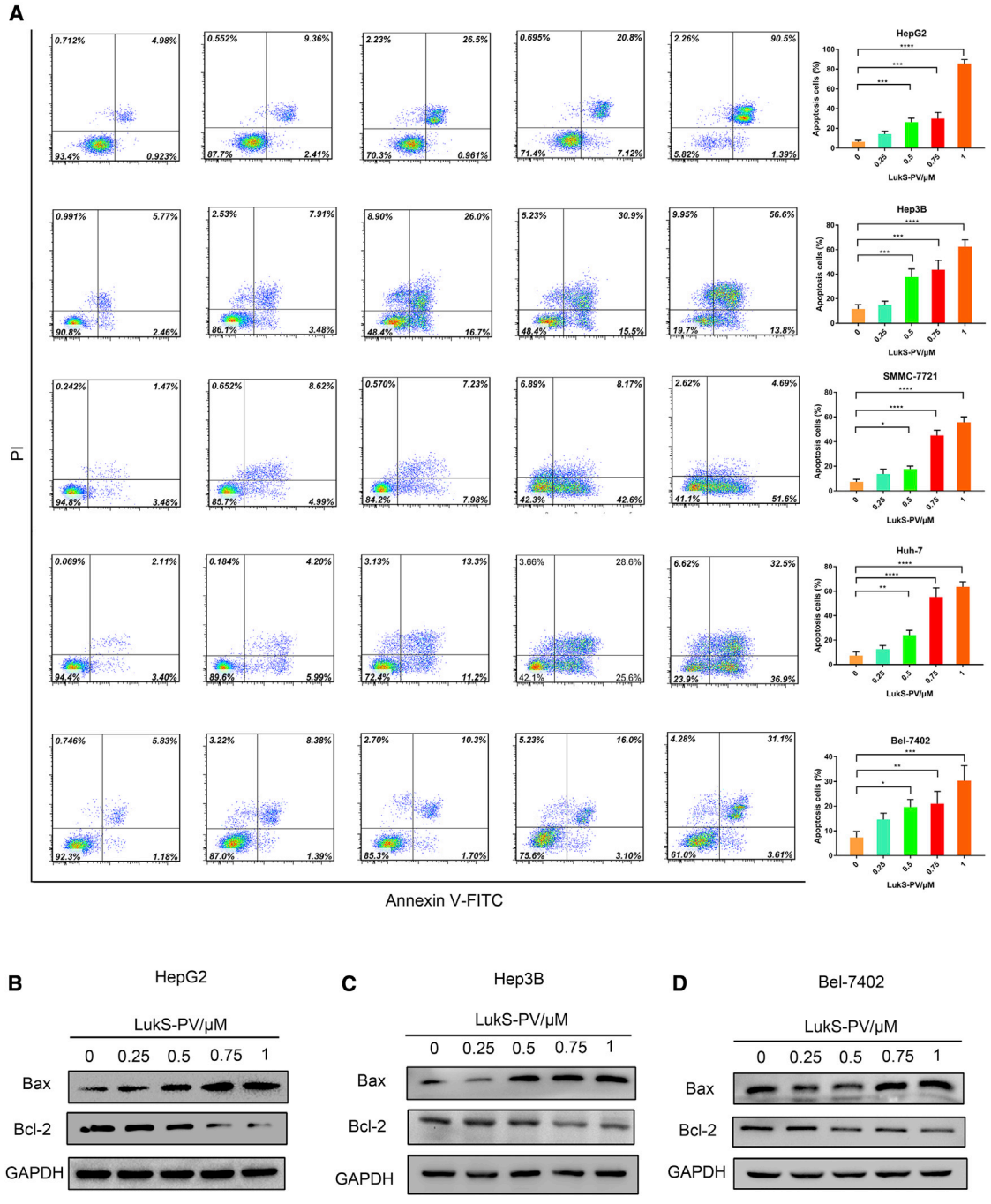

Figure 2. LukS-PV Induced Apoptosis in HCC Cells that Express C5aR

(A) Cell apoptosis in HCC cells treated with different concentrations of LukS-PV was examined by flow cytometry. (B) The protein expression levels of Bax and Bcl-2 were detected in HepG2 cells treated with different concentrations of LukS-PV. (C) The protein expression levels of Bax and Bcl-2 were detected in Hep3B cells treated with different concentrations of LukS-PV. (D) The protein expression levels of Bax and Bcl-2 were detected in Bel-7402 cells treated with different concentrations of LukS-PV.

LukS-PV Induced Cell-Cycle Arrest in HCC Cells

To study the effect of LukS-PV on the cell-cycle progression of liver cancer cells, we treated cells with different concentrations of LukS-PV for 24 h. Flow cytometry results showed that LukS-PV induced cell-cycle arrest at the G0/G1 phase in HCC cells (Figures 3A–3F). To further investigate the mechanism, we used qRT-PCR to detect mRNA expression of p21, cycinA2, and cycinD1. The results showed that LukS-PV increased p21 expression and

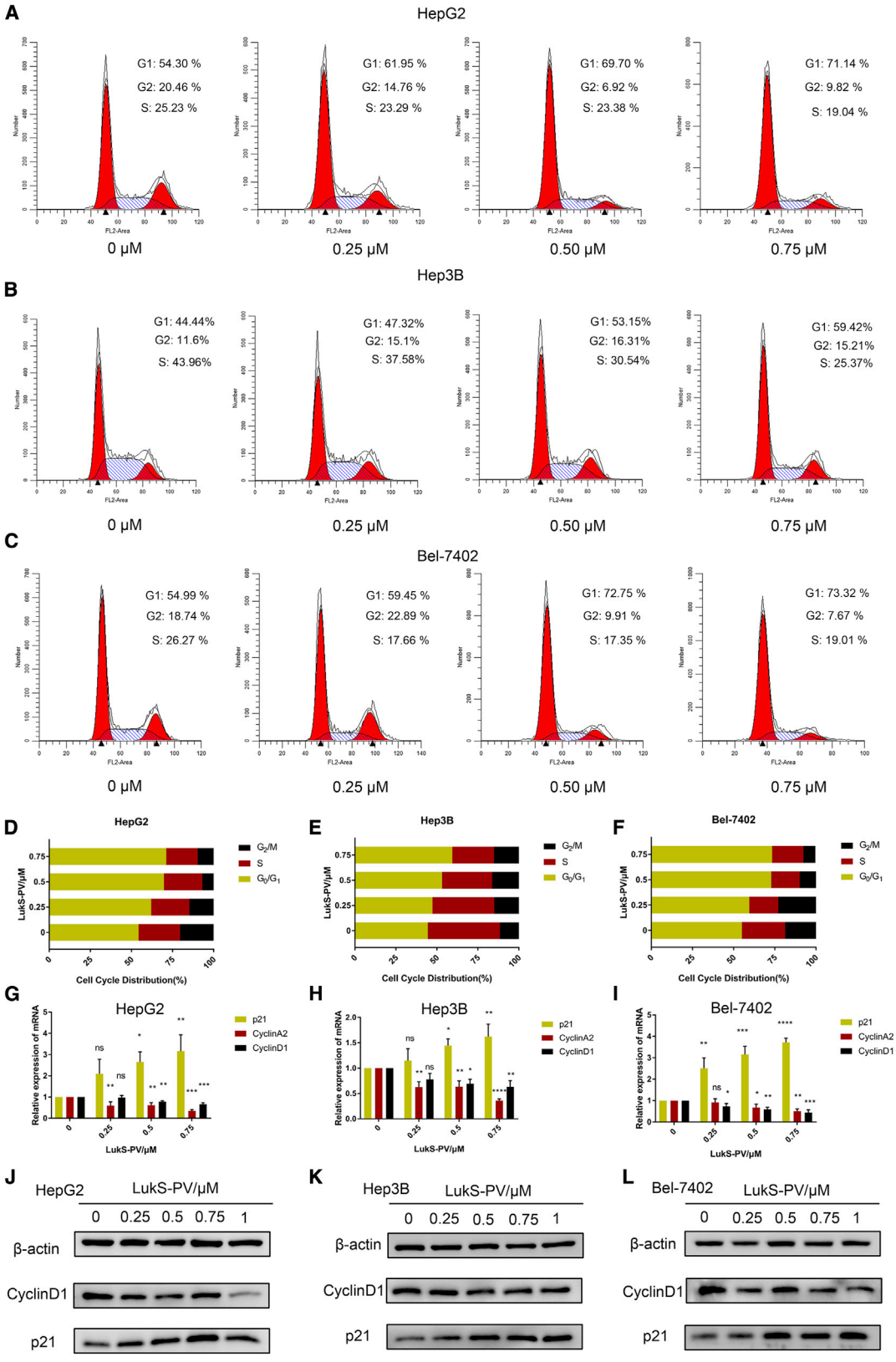

(legend on next page)

decreased the expression of cycinA2 and cycinD1 (Figures 3G–3I). Furthermore, we measured protein levels of Cyclin D1 and p21. As presented in Figures 3J–3L, LukS-PV increased p21 protein levels and Cyclin D1 levels. Taken together, these results indicated that LukS-PV induced cell-cycle arrest in HCC cells.

LukS-PV Downregulated HDAC2 in HCC Cells

To understand the potential mechanism through which LukS-PV exerted antitumor effects in HCC, we employed RNA sequencing and quantitative proteomics sequencing to uncover the transcriptional and proteomic alterations in HepG2 cells after PBS or LukS-PV treatment. Intriguingly, we found that HDAC2 was downregulated in the LukS-PV treatment group (Figures 4A and 4B). Furthermore, we verified that HDAC2 was downregulated by LukS-PV using qRT-PCR and western blot in HCC cells (Figures 4C–4E). Collectively, these data revealed that LukS-PV decreased HDAC2 expression in HCC cells.

LukS-PV Inhibited the Proliferation of HCC Cells by Downregulating HDAC2 Expression

To further determine whether LukS-PV inhibited the proliferation of HCC cells through HDAC2, we first examined HDAC2 expression in HCC cell lines and the normal hepatocyte cell line L02. qRT-PCR and western blot results showed that HDAC2 expression was significantly increased in HCC cells (Figures 5A and 5B). Meanwhile, we also found that the expression of HDAC2 in HepG2 cells was higher and the expression of HDAC2 in Bel-7402 was lower (Figures 5A and 5B). Therefore, HepG2 cells were selected to knock down the expression of HDAC2, and Bel-7402 cells were selected to perform overexpression and rescue experiment. To explore the functional role of HDAC2, we knocked down HDAC2 in HepG2 cells. Small interfering RNA (siRNA)-mediated knockdown of HDAC2 resulted in a dramatic decrease in the proliferation of HepG2 cells (Figure 5C). In contrast, ectopic expression of HDAC2 led to a marked increase in the proliferation of Bel-7402 cells (Figure 5D), and ectopic expression of HDAC2 significantly attenuated the inhibitory effects of LukS-PV on the proliferation of Bel-7402 cells compared with that of the LukS-PV treatment group (Figure 5D). The similar effect was reproduced by EdU assay (Figures 5E–5H). These results indicated that LukS-PV inhibited the proliferation of HCC cells by downregulating HDAC2 expression.

LukS-PV Induced Cell Apoptosis and Cell-Cycle Arrest in HCC Cells by Downregulating HDAC2 Expression

To study the role of HDAC2 on cell apoptosis and cell-cycle arrest in HCC cells, we used flow cytometry to detect apoptotic cells and analyze cell-cycle distribution. As illustrated in Figures 6A and 6B, HepG2 cells transfected with HDAC2 siRNA for 48 h had increased the apoptosis rate and G0/G1 populations. Ectopic expression of HDAC2 in Bel-7402 cells was shown to raise the rate of apoptosis cells and accelerate cell-cycle progression (Figures 6C and 6D). In addition, the effects of LukS-PV on cell apoptosis and cell-cycle arrest could be markedly reversed by ectopically expressed HDAC2 (Figures 6C and 6D). In accordance, HDAC2 knockdown was able to increase protein levels of Bax and p21, and decrease protein levels of Bcl-2 and Cyclin D1 (Figure 6E). Overexpressing HDAC2 elevated the protein expression of Bax and p21 but reduced the protein expression of Bcl-2 and Cyclin D1 (Figure 6F). Similarly, the effect of LukS-PV on apoptosis-related proteins and cycle-related proteins can be reversed by HDAC2 overexpression (Figure 6F). These results indicated that LukS-PV induced cell apoptosis and cell-cycle arrest in HCC cells by downregulating HDAC2 expression.

LukS-PV Increased PTEN Expression and Decreased AKT Phosphorylation via HDAC2

To explore the molecular mechanism through which downregulating HDAC2 inhibited HCC progression, we performed RNA sequencing. The results indicated that LukS-PV led to the upregulation of 1,678 genes and the downregulation of 1,008 genes compared with the PBS group (Figure 7A). After running the differentially expressed genes through the Kyoto Encyclopedia of Genes and Genomes (KEGG) and Gene Set Enrichment Analysis (GSEA) pathway analysis, the phosphatidylinositol 3-kinase (PI3K)/AKT signaling pathway attracted our attention (Figures 7B and 7C). Furthermore, we found that PTEN was upregulated after LukS-PV treatment in the RNA sequencing data (Figure 7A). Therefore, we hypothesized that LukS-PV might increase PTEN expression and decrease AKT phosphorylation via HDAC2. qRT-PCR and western blot analyses revealed that compared with the control group, the LukS-PV group had significantly increased PTEN mRNA and protein levels in HCC cells (Figures 7D–7G). It was also demonstrated that LukS-PV did not affect total AKT protein levels; however, AKT phosphorylation decreased compared with the control group after LukS-PV treatment for 24 h (Figures 7E–7G). Furthermore, we investigated the role of HDAC2 in the PTEN/AKT pathway. As shown in Figures 7H and 7J, PTEN expression in the HDAC2-silenced group was increased compared with the negative control group. Levels of phosphorylated AKT (p-AKT) were also markedly decreased in the HDAC2-silenced group compared with the negative control. By overexpressing HDAC2 gene in Bel-7402 cells, the mRNA and protein expression

Figure 3. LukS-PV Induced Cell-Cycle Arrest in HCC Cells

(A) Cell-cycle distribution in HepG2 cells with different concentrations of LukS-PV was examined by flow cytometry. (B) Cell-cycle distribution in Hep3B cells with different concentrations of LukS-PV was examined by flow cytometry. (C) Cell-cycle distribution in Bel-7402 cells with different concentrations of LukS-PV was examined by flow cytometry. (D) Percentagess of different cell cycles were calculated in HepG2 cells. (E) Percentagess of different cell cycles were calculated in Hep3B cells. (F) Percentagess of different cell cycles were calculated in Bel-7402 cells. (G) The mRNA expression levels of p21, Cyclin A2, and Cyclin D1 were detected in HepG2 cells with different concentrations of LukS-PV. (H) The mRNA expression levels of p21, Cyclin A2, and Cyclin D1 were detected in Hep3B cells with different concentrations of LukS-PV. (I) The mRNA expression levels of p21, Cyclin A2, and Cyclin D1 were detected in Bel-7402 cells with different concentrations of LukS-PV. (J) The protein expression levels of p21 and Cyclin D1 were detected in HepG2 cells with different concentrations of LukS-PV. (K) The protein expression levels of p21 and Cyclin D1 were detected in Hep3B cells with different concentrations of LukS-PV. (L) The protein expression levels of p21 and Cyclin D1 were detected in Bel-7402 cells with different concentrations of LukS-PV.

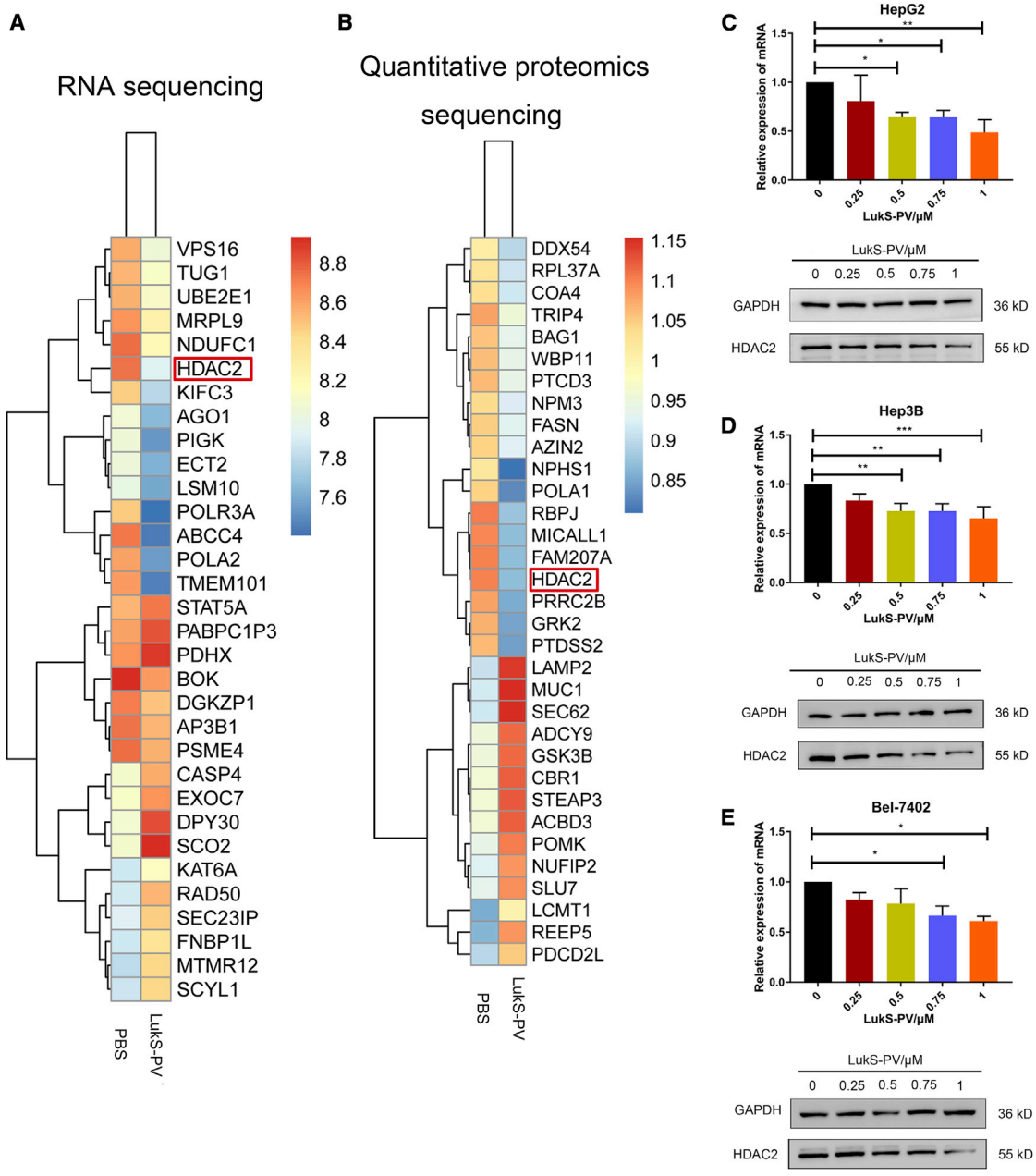

Figure 4. LukS-PV Downregulated HDAC2 in HCC Cells

(A) RNA sequencing was performed to identify the change of HDAC2 expression level in HepG2 cells treated with LukS-PV or PBS. (B) Quantitative proteomics sequencing was performed to identify the change of HDAC2 expression level in HepG2 cells treated with LukS-PV or PBS. (C) The mRNA and protein expression levels of HDAC2 were detected in HepG2 cells treated with different concentrations of LukS-PV. (D) The mRNA and protein expression levels of HDAC2 were detected in Hep3B cells treated with different concentrations of LukS-PV. (E) The mRNA and protein expression levels of HDAC2 were detected in Bel-7402 cells treated with different concentrations of LukS-PV.

of PTEN were decreased, and the protein expression of p-AKT was increased (Figures 7I and 7K). The effect of LukS-PV on PTEN and p-AkT can be reversed by HDAC2 overexpression (Figures 7I and 7K). Overall, these data suggest that LukS-PV increases PTEN expression and decreases AKT phosphorylation via HDAC2. However, it is not clear how HDAC2 regulates PTEN. We identified the putative miR-3691-5p binding sites in the PTEN 3′ UTR by using TargetScan database (http://www.targetscan.org/vert_72/) (Figure 7L). Also, Du et al.[32] demonstrated that PTEN is a direct target of miR-3691-5p in HCC. Based on this, we wondered whether LukS-PV could downregulate miR-3691-5p by downregulating HDAC2. As shown in Figure 7M, we proved that LukS-PV could downregulate the expression

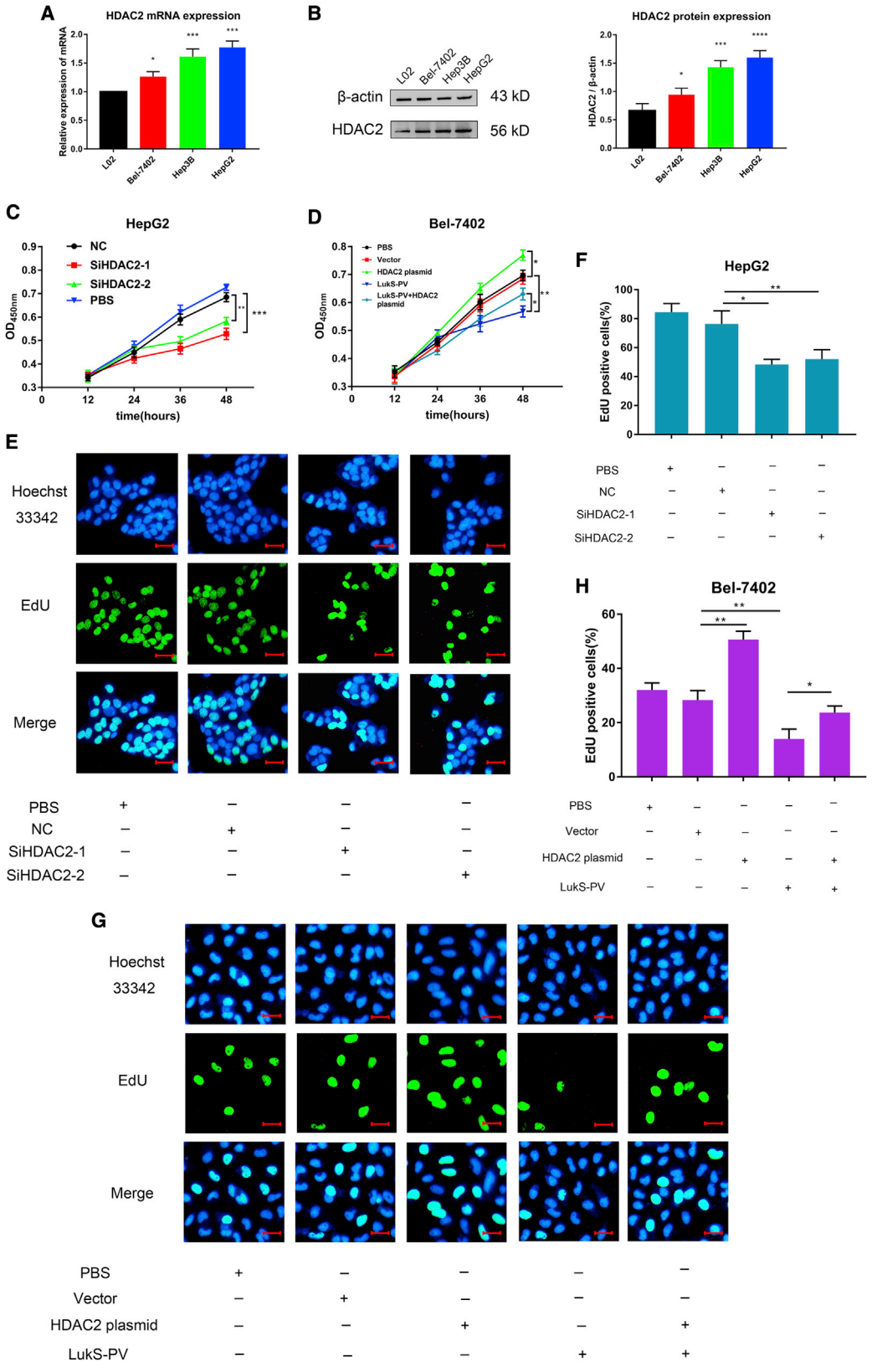

(legend on next page)

of miR-3691-5p in HCC cells. HDAC2 silence with siRNAs decreased the expression of miR-3691-5p (Figure 7N). Accordingly, we increased HDAC2 expression in Bel-7402 cells, and results revealed that HDAC2 overexpression increased the expression of miR-3691-5p (Figure 7O). The rescue experiment results showed that overexpression of HDAC2 could abrogate the inhibitory effect of LukS-PV in Bel-7402 cells (Figure 7O).

LukS-PV Inhibited Liver Cancer Progression *In Vivo*

Given that LukS-PV inhibited the growth of HCC cells *in vitro*, we next performed animal experiments to investigate whether LukS-PV inhibited liver cancer progression *in vivo*. Using a xenograft mouse model, we found that LukS-PV inhibited tumor growth in nude mice (Figures 8A–8D). Hematoxylin and eosin (H&E) staining showed large necrotic areas in tumor tissues after LukS-PV treatment (Figure 8E). Additionally, immunohistochemistry (IHC) showed that LukS-PV reduced Ki-67 and HDAC2 expression compared with the control group (Figures 8F and 8G). Taken together, these findings suggested that LukS-PV had antitumor activity *in vivo*. To further confirm the role of HDAC2 in liver cancer, we used ULACAN[33] to analyze HDAC2 expression in liver cancer in cases from The Cancer Genome Atlas (TCGA) database. These data showed a dramatic increase in HDAC2 expression in tumor samples compared with normal tissues. Furthermore, HDAC2 was closely associated with the clinicopathological stage of liver cancer (Figures 8H and 8I). Finally, patients with high HDAC2 expression had reduced overall survival compared with the low HDAC2 expression group (Figure 8J). These results showed that HDAC2 could be a prognostic marker for liver cancer.

DISCUSSION

Liver cancer is a common tumor of the digestive tract, and its incidence rate is increasing annually.[34] Currently, the recognized pathogenesis of liver cancer is transformation due to inflammation, such as hepatitis B infection. It has been reported that approximately 75% of liver cancer patients have hepatitis B infection.[35] Thus, inflammation plays an important role in liver cancer development. The complement system is an important component of the inflammatory response. C5aR is a receptor for complement C5a. Recently, it was found that C5aR is highly expressed in many tumors, and that high C5aR expression is related to tumor size, invasion, and metastasis.[15–19] Our previous study found that LukS-PV had anti-leukemia effects that were mediated by C5aR.[14] In this study, we found that LukS-PV inhibited proliferation and induced apoptosis of HCC cells with high C5aR expression.

Bacterial toxins that can target and kill cancer cells have been used in clinical research.[5] In previous studies, we found that LukS-PV can inhibit leukemia cell proliferation and induce cell-cycle arrest and apoptosis.[13] Here, we confirmed that LukS-PV could also inhibit the proliferation of HCC cells by cell viability and EdU assays. Intriguingly, the cell viability assay showed that the inhibition rate was positively correlated with C5aR expression. Furthermore, the effect of LukS-PV on apoptosis in HCC cells was studied, and the apoptosis rate was related to C5aR expression. This result underscores the significance of C5aR expression in LukS-PV treatment. Regarding the mechanism of apoptosis in leukemia cells, it was found by gene chip detection that LukS-PV induced apoptosis in leukemia cells primarily through the mitochondrial pathway. In this study, we also found that mitochondrial apoptosis pathway-associated proteins were significantly increased after treatment, indicating that LukS-PV induced apoptosis in HCC cells through the mitochondrial pathway. Moreover, LukS-PV was proved to block cell-cycle progression in HCC cells at the G0/G1 phase. To clarify the underlying mechanism, we detected several cell-cycle regulatory proteins. This analysis showed that LukS-PV increased the levels of p21, while simultaneously decreasing the levels of Cyclin D1. Overall, we demonstrated that LukS-PV inhibited HCC progression by inhibiting proliferation and inducing apoptosis and cell-cycle arrest.

Acetylation has been confirmed to play a vital role in the onset and progression of tumors. Therefore, we searched for relevant targets involved in acetylation regulation by performing RNA sequencing and quantitative proteomics sequencing. Indeed, HDAC2 attracted our attention, because it was downregulated in the LukS-PV treatment group both in RNA sequencing and in quantitative proteomics sequencing. HDACs are often abnormally overexpressed in a variety of tumors. HDAC overexpression disrupts normal cell-cycle progression and differentiation, and HDAC2 is one of the most frequently overexpressed HDACs in tumors.[36,37] Monitoring HDAC2 expression during treatment can serve as a marker of HDAC inhibitor efficacy, and HDAC2 expression levels represent independent clinical prognostic markers.[38,39] Thus, qRT-PCR and western blot were used to verify the decreased expression of HDAC2.

Given that HDAC2 plays a pivotal role in tumors, we hypothesized that LukS-PV may inhibit HCC progression by downregulating HDAC2. Therefore, we examined the effects of HDAC2 knockdown or overexpression on the proliferation, apoptosis, and cell-cycle progression of HCC cells using HDAC2-specific siRNA or HDAC2

Figure 5. LukS-PV Inhibited the Proliferation of HCC Cells by Downregulating HDAC2 Expression

(A) qRT-PCR was applied to detect endogenous mRNA levels of HDAC2 in L02 and HCC cells. (B) Western blot was applied to detect endogenous protein levels of HDAC2 in L02 and HCC cells. (C) HepG2 cells were infected with negative control (NC), siHDAC2-1, or siHDAC-2. Forty-eight hours later, the cell growth curves were measured by counting cell numbers at the indicated time points. (D) Bel-7402 cells were treated with PBS, Vector, HDAC2 plasmid, LukS-PV, or both LukS-PV and HDAC2 plasmid. Forty-eight hours later, the cell growth curves were measured by counting cell numbers at the indicated time points. (E) HepG2 cells were infected with NC, siHDAC2-1, or siHDAC-2. Forty-eight hours later, cells were subjected to EdU assay. (F) EdU positive cells were calculated in HepG2 cells. (G) Bel-7402 cells were treated with PBS, Vector, HDAC2 plasmid, LukS-PV, or both LukS-PV and HDAC2 plasmid. Forty-eight hours later, cells were subjected to EdU assay. (H) EdU positive cells were calculated in Bel-7402 cells. Scale bars, 20 μm.

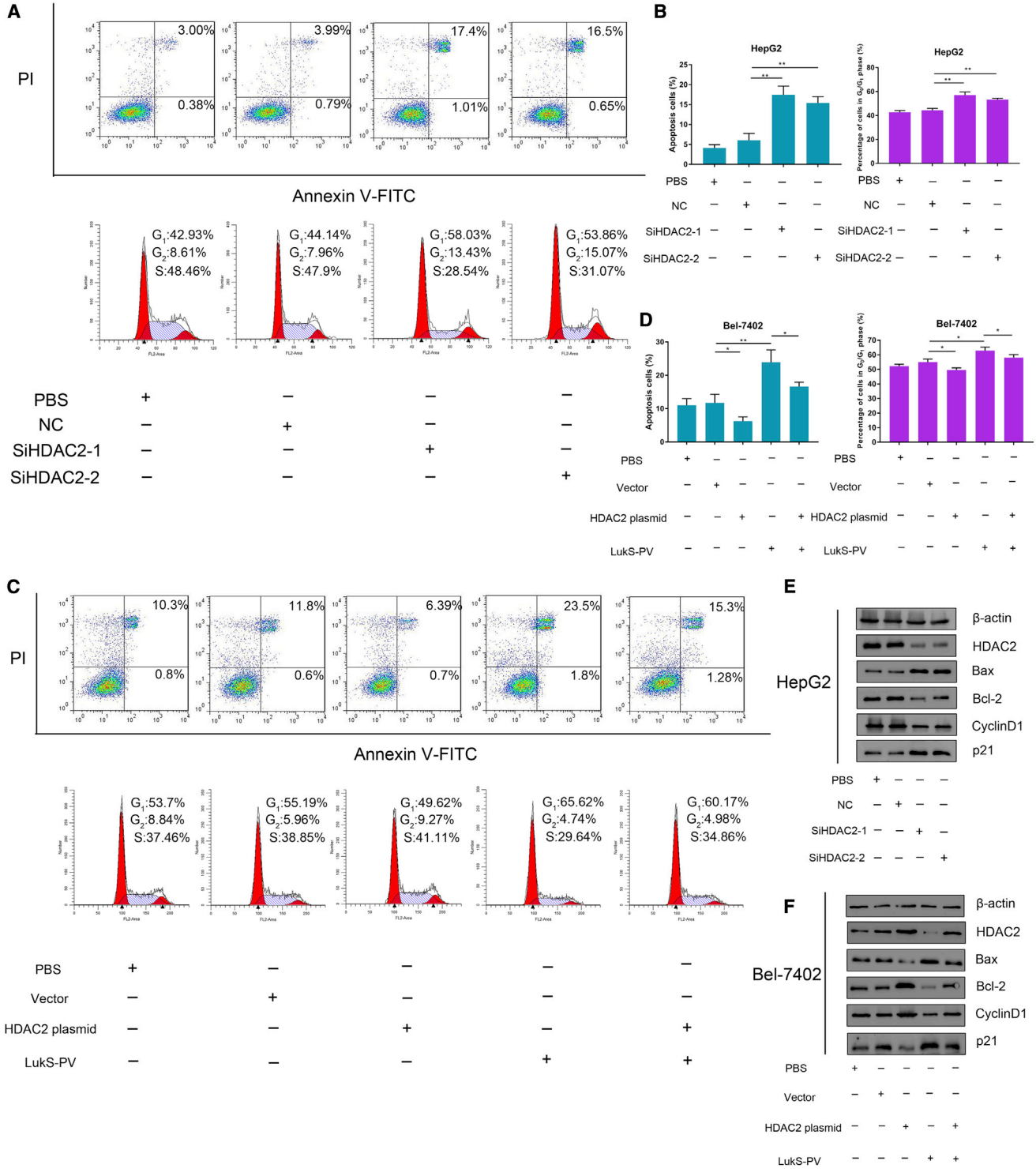

Figure 6. LukS-PV Induced Cell Apoptosis and Cell-Cycle Arrest in HCC Cells by Downregulating HDAC2 Expression

(A) HepG2 cells were infected with NC, siHDAC2-1, or siHDAC-2. Forty-eight hours later, cells were subjected to cell apoptosis and cell-cycle arrest assay. (B) Apoptosis cells and percentage of G_0/G_1 phase cells were calculated in HepG2 cells. (C) Bel-7402 cells were treated with PBS, Vector, HDAC2 plasmid, LukS-PV, or both LukS-PV and HDAC2 plasmid. Forty-eight hours later, cells were subjected to cell apoptosis and cell-cycle arrest assay. (D) Apoptosis cells and percentage of G_0/G_1 phase cells were calculated in Bel-7402 cells. (E) HepG2 cells were infected with NC, siHDAC2-1, or siHDAC-2. Forty-eight hours later, the protein expression

(legend continued on next page)

plasmid. We verified that silencing HDAC2 significantly decreased proliferation, induced apoptosis, and blocked cell-cycle progression. Accordingly, ectopic expression of HDAC2 in Bel-7402 cells was shown to promote cell proliferation, raise the rate of apoptosis cells, and accelerate cell-cycle progression. Results of rescue experiment revealed that overexpression of HDAC2 could abrogate the inhibitory effect of LukS-PV on HCC cells. Lee et al.[40] found that HDAC2 knockdown arrested the cell cycle in the G0/G1 phase, which was similar to our data. In this study, we found that HDAC2 expression was downregulated by LukS-PV, and that LukS-PV caused cell-cycle arrest in the G0/G1 phase, indicating that LukS-PV may affect cell-cycle progression by limiting HDAC2 expression. Thus, we conclude that LukS-PV downregulates HDAC2 expression to inhibit HCC progression.

To uncover the underlying mechanism of how LukS-PV inhibited HCC progression via HDAC2, we performed the enrichment analysis on RNA sequencing data. According to KEGG and GSEA pathway analysis, the PI3K/AKT pathway was altered in treated cells. The PI3K/AKT pathway is a primary intracellular signaling cascade that is closely related to cell growth, proliferation, and survival. Numerous studies have indicated that the PI3K/AKT pathway is overactivated in many malignancies, where it promotes cell growth, proliferation, and angiogenesis. HDACs can not only affect the acetylation of histones, but also the acetylation of other proteins. PTEN expression was found to be upregulated in RNA sequencing data. PTEN is a tumor suppressor gene that can inhibit cell proliferation and induce apoptosis.[41] Studies have shown that downregulation of HDAC2 can increase the expression of the tumor suppressor PTEN.[42] Pan et al.[43] found that trichostatin A inhibited the expression of HDAC and upregulated the expression of PTEN. The mechanism for this activity may be that TSA upregulated PTEN through an important transcription factor Egr-1 and enhancing acetylation of the PTEN promoter, leading to the upregulation of PTEN. Importantly, Bian et al.[44] reported that AKT was a downstream target of PTEN, and that AKT phosphorylation was suppressed by PTEN. Therefore, we hypothesized that LukS-PV may downregulate HDAC2, which inhibited HCC progression through the PTEN/AKT pathway. In this study, we first found that LukS-PV upregulated PTEN expression and decreased p-AKT levels. Knockdown, overexpression, and rescue experiment were used to prove that LukS-PV increased PTEN expression and decreased AKT phosphorylation via HDAC2. However, it has not yet been clarified how HDAC2 regulates PTEN. miRNAs are known to play a critical and functional role in a broad range of key molecular processes via sophisticated regulation of distinct targets, orchestrating a molecular intracellular balance of gene expression. Conte et al.[45] identified a cluster of common upregulated and downregulated miRNAs in both SAHA-treated and HDAC2 downregulated cells in AML. Du et al.[32] demonstrated that PTEN is a direct target of miR-3691-5p in HCC, and miR-3691-5p expression was elevated in both HCC tissues and cell lines, which was significantly correlated with poor prognosis and clinicopathological features. So we wondered whether LukS-PV could downregulate miR-3691-5p by downregulating HDAC2. Subsequently, qRT-PCR was used to verify that LukS-PV could downregulate the expression of miR-3691-5p in HCC cells. Results of knockdown, overexpression, and rescue experiment implied that LukS-PV could downregulate the expression of miR-3691-5p via HDAC2 in HCC cells. Overall, LukS-PV decreased the expression of miR-3691-5p by downregulating HDAC2. Furthermore, the reduced miR-3691-5p bound to the 3′ UTR of PTEN, and the expression of PTEN was downregulated.

Finally, we investigated whether LukS-PV could inhibit the progression of liver cancer *in vivo*. As expected, the rate of tumor growth in the LukS-PV group was significantly decreased. Meanwhile, IHC results confirmed decreased HDAC2 and Ki-67 expression. This indicated that HDAC2 was a crucial target of LukS-PV. In fact, HDAC2 is overexpressed and serves as a considerable risk factor in liver cancer according to analysis of TCGA data. Together, these findings suggested that LukS-PV may repress liver cancer progression *in vivo* by downregulating HDAC2, which plays a significant role in HCC onset and progression.

In conclusion, this study demonstrated that LukS-PV increased PTEN expression and decreased AKT phosphorylation via HDAC2, thereby inhibiting the proliferation of HCC cells and inducing apoptosis and cell-cycle arrest (Figure 8K).

MATERIALS AND METHODS

Production and Purification of Recombinant LukS-PV

The LukS-PV sequence was amplified from PVL-positive *Staphylococcus aureus* isolates by PCR. Purification of recombinant LukS-PV was performed with the His-Bind Purification Kit (Millipore, USA) according to the manufacturer's instructions.

Cell Culture

The human HCC cell lines HepG2, Bel-7402, Hep3B, Huh7, and SMMC-7721, and the normal liver cell line L02 were purchased from Shanghai Cell Bank of Chinese Academy of Sciences. Bel-7402, SMMC-7721, and L02 cells were cultured in RPMI-1640 (GIBCO, USA) supplemented with 10% fetal bovine serum, 100 U/mL penicillin, and 100 mg/mL streptomycin. HepG2, Hep3B, and Huh7 cells were cultured in DMEM (GIBCO, USA) supplemented with 10% fetal bovine serum, 100 U/mL penicillin, and 100 mg/mL streptomycin. Cells were maintained in a humidified incubator with 5% CO_2.

levels of HDAC2, Bax, Bcl-2, Cyclin D1, and p21 were detected. (F) Bel-7402 cells were treated with PBS, Vector, HDAC2 plasmid, LukS-PV, or both LukS-PV and HDAC2 plasmid. Forty-eight hours later, the protein expression levels of HDAC2, Bax, Bcl-2, Cyclin D1, and p21 were detected.

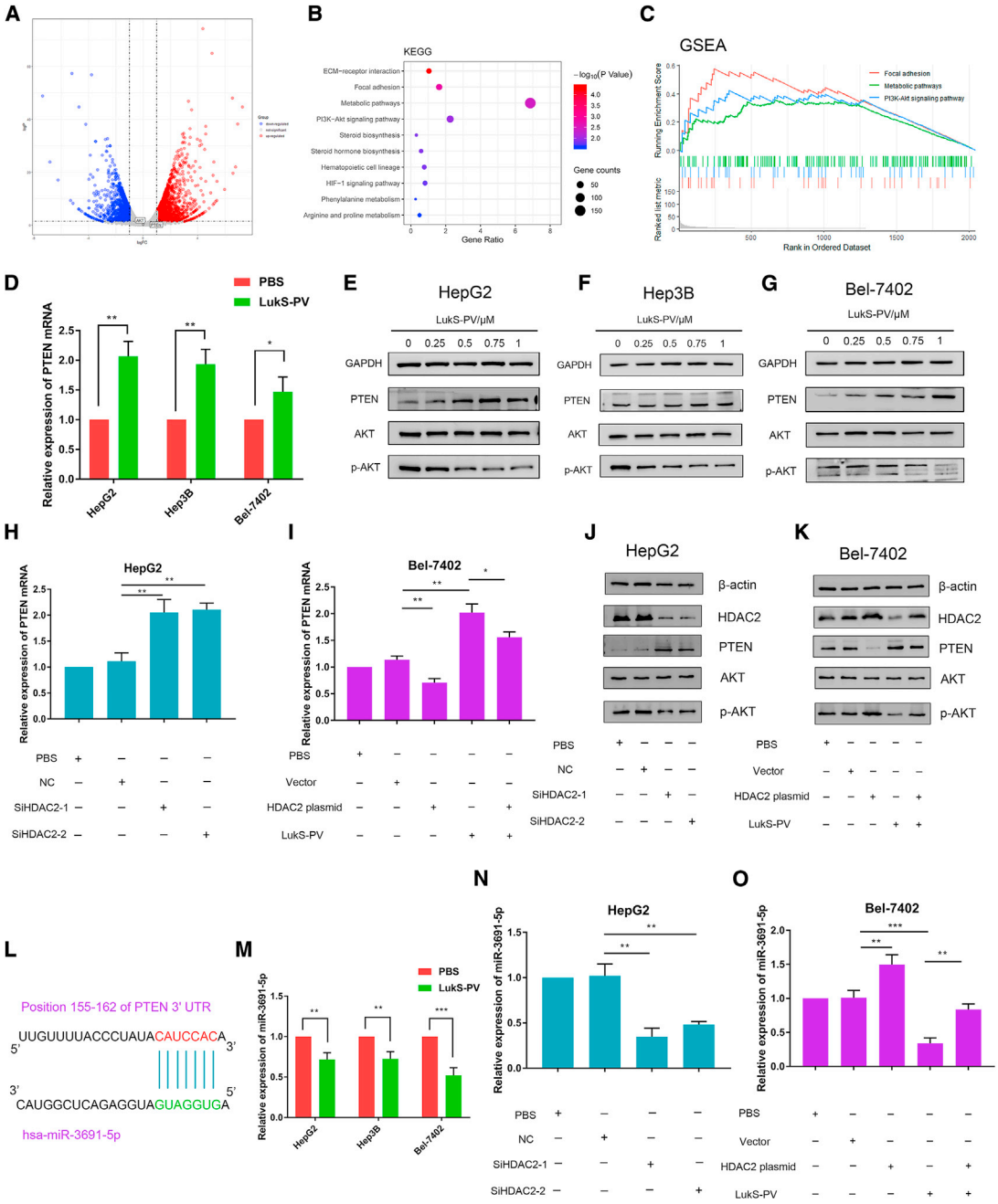

Figure 7. LukS-PV Increased PTEN Expression and Decreased AKT Phosphorylation via HDAC2

(A) The volcano map shows the difference gene in HepG2 cells treated with PBS or LukS-PV by RNA sequencing. AKT and PTEN are labeled in the map. (B) KEGG pathway enrichment analysis revealed the signaling pathways potentially involved in LukS-PV functions. (C) GSEA pathway enrichment analysis revealed the signaling pathways potentially involved in LukS-PV functions. (D) The mRNA expression levels of PTEN were detected in HCC cells with LukS-PV. (E) The protein expression levels of PTEN, AKT, and p-AKT were detected in HepG2 cells with different concentrations of LukS-PV. (F) The protein expression levels of PTEN, AKT, and p-AKT were detected in Hep3B cells with different concentrations of LukS-PV. (G) The protein expression levels of PTEN, AKT, and p-AKT were detected in Bel-7402 cells with different concentrations of LukS-PV. (H) HepG2 cells were infected with NC, siHDAC2-1, or siHDAC-2. Forty-eight hours later, the mRNA levels of PTEN were detected. (I) Bel-7402 cells were treated with PBS, Vector, HDAC2 plasmid, LukS-PV, or both LukS-PV and HDAC2 plasmid. Forty-eight hours later, the mRNA levels of PTEN were detected. (J) HepG2 cells were infected with NC, siHDAC2-1, or siHDAC-2. Forty-eight hours later, the protein expression levels of HDAC2, PTEN, AKT, and p-AKT were detected. (K) Bel-7402 cells were treated with PBS, Vector, HDAC2 plasmid, LukS-PV, or both LukS-PV and HDAC2 plasmid. Forty-eight hours later, the protein expression levels of HDAC2, PTEN, AKT, and p-AKT were detected. (L) miR-3691-5p and its putative binding sequence in the 3′ UTR of PTEN by using TargetScan database. (M) The miR-3691-5p expression levels were

(legend continued on next page)

Cell Proliferation Assay

Cells were seeded in 96-well plates (5,000 cells/well) and treated with different concentrations of LukS-PV, plasmid, or siRNA at 37°C for 24 h. Then 10 μL of Cell Counting Kit-8 reagent (BIOMIKY, China) was added to each well, and the plates were incubated at 37°C for 2 h. Finally, the absorbance of each well was measured at 450 nm using a microplate reader.

EdU Assay

The proliferation capacity of HCC cells after transfection with siRNA, plasmid, or treatment with LukS-PV was detected using an EdU kit (keyGEN, China). EdU was labeled with kFluor488, which appears as green fluorescence. Cells were seeded at 5,000 cells/well in 96-well plates and incubated with LukS-PV or siRNA for 24 h. Then 50 nM EdU working solution was added and incubated for 2.5 h. Hoechst 33342 was used to counterstain nuclei for 30 min in the dark. Finally, EdU-positive cells were observed and counted under a fluorescence microscope.

Cell-Cycle Analysis

HCC cells treated with LukS-PV or transfected with siRNA or plasmid were harvested for cell-cycle analysis using the Cell Cycle Assay Kit (keyGEN, China). The cells were stained with propidium iodide and treated with RNase A for 30 min in the dark. Finally, the cells were subjected to flow cytometry using a BD FACSCalibur. The percentages of cells in different cell-cycle phases were calculated using ModFit 5.0.

Apoptosis Assay

HCC cells treated with LukS-PV or transfected with siRNA or plasmid were harvested and analyzed for apoptosis using the Apoptosis Assay Kit (keyGEN, China). Cells were treated with fluorescein isothiocyanate (FITC)-Annexin V and propidium iodide in the dark at room temperature. Finally, the cells were analyzed on a BD FACSCalibur.

Quantitative Reverse Transcriptase PCR

Cells were subjected to RNA extraction using TRIzol reagent (Invitrogen, USA). qRT-PCR was performed with a Roche LightCycler 480 using SYBR Green Master Mix (Takara, China) according to the manufacturer's instructions. The relative mRNA expression levels of investigated genes were normalized to GAPDH using the $2^{-\Delta\Delta Ct}$ method. All experiments were performed in triplicate. The primer pairs of qRT-PCR were as follows: GAPDH (5′-GGA GCG AGA TCC CTC CAA AAT-3′ and 5′-GGC TGT TGT CAT ACT TCT CAT GG-3′), HDAC2 (5′-ATG GCG TAC AGT CAA GGA GG-3′ and 5′-TGC GGA TTC TAT GAG GCT TCA-3′), PTEN (5′-TTT GAA GAC CAT AAC CCA CCAC-3′ and 5′-ATT ACA CCA GTT CGT CCC TTT C-3′), Cyclin A2 (5′-GGA TGG TAG TTT TGA GTC ACC AC-3′ and 5′-CAC GAG GAT AGC TCT CAT ACT GT-3′), Cyclin D1 (5′-GCT GCG AAG TGG AAA CCA TC-3′ and 5′-CCT CCT TCT GCA CAC ATT TGA A-3′), and p21 (5′-TGT CCG TCA GAA CCC ATG C-3′ and 5′-AAA GTC GAA GTT CCA TCG CTC-3′). The primers of U6 and miR-3691-5p were purchased from Genecopoeia.

Western Blot Assay

Proteins were separated on 10% SDS-PAGE gels and transferred to nitrocellulose membranes. Membranes were blocked with 5% bovine serum albumin and incubated with the indicated primary antibodies. Corresponding horseradish peroxidase-conjugated secondary antibodies were used following primary antibody incubation. The primary antibodies used were as follows: anti-HDAC2 (Proteintech, China), anti-Bax (Cell Signaling Technology, USA), anti-Bcl-2 (Cell Signaling Technology, USA), anti-CyclinD1 (Cell Signaling Technology, USA), anti-p21 (Cell Signaling Technology, USA), anti-Pan-acetylation (PTM Biolabs China), anti-C5aR (Abcam, USA), anti-PTEN (Proteintech, China), anti-AKT (Cell Signaling Technology, USA), anti-p-AKT (Cell Signaling Technology, USA), anti-GAPDH (Abclonal, China), and anti-β-actin (Abclonal, China).

Transfection

HDAC2 plasmid, siRNA-HDAC2, and corresponding negative control vector were purchased from GenePharma. HCC cells were transfected with siRNA or plasmid at a final concentration of 50 nmol/L using Lipofectamine 2000 (Invitrogen, USA). Transfection efficiency was assessed by qRT-PCR and western blot. The primer sequence of transfection was as follows: negative control (sense: 5′-UUC UCC GAA GGU GUC ACG UTT-3′; antisense: 5′-ACG UGA CAC GUU CGG AGA ATT-3′), HDAC2-1 (sense: 5′-GCA AAU ACU AUG CUG UCA ATT-3′; antisense: 5′-UUG ACA GCA UAG UAU UUG CTT-3′), and HDAC2-2 (sense: 5′-CCA GAA CAC UCC AGA AUA UTT-3′; antisense: 5′-AUA UUC UGG AGU GUU CUG GTT-3′).

RNA Sequencing

Total RNA of HepG2 cells treated with LukS-PV or PBS was isolated using the RNeasy mini kit (QIAGEN, Germany). Paired-end-libraries were synthesized by using the TruSeq™ RNA Sample Preparation Kit(Illumina, USA) following TruSeq™ RNA Sample Preparation Guide. Briefly, The poly-A containing mRNA molecules were purified using poly-T oligo-attachedmagnetic beads. Library construction and sequencing were performed at Shanghai Sinomics Corporation.

detected in HCC cells with LukS-PV. (N) HepG2 cells were infected with NC, siHDAC2-1, or siHDAC-2. Forty-eight hours later, the miR-3691-5p expression levels were detected. (O) Bel-7402 cells were treated with PBS, Vector, HDAC2 plasmid, LukS-PV, or both LukS-PV and HDAC2 plasmid. Forty-eight hours later, the miR-3691-5p expression levels were detected.

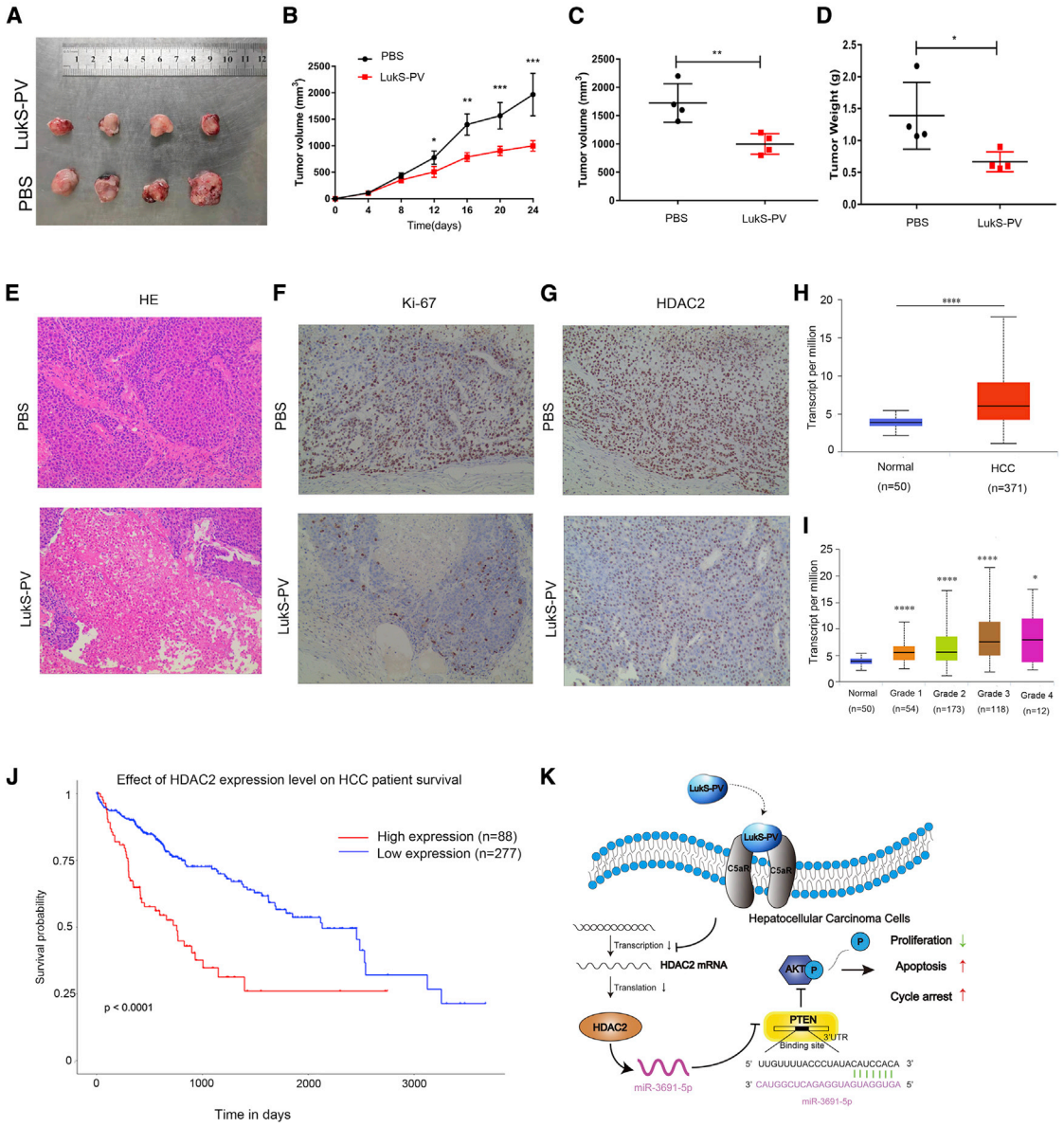

Figure 8. LukS-PV Inhibited Liver Cancer Progression *In Vivo*

(A) The size of tumors separated from nude mice treated with PBS or LukS-PV. (B) The growth curve of tumor volumes treated with PBS or LukS-PV. (C) Tumor volume was measured and calculated. (D) Tumor weight was measured and calculated. (E) Representative pictures of H&E staining for tumor models. (F) Representative pictures of IHC staining of Ki-67 for tumor models. (G) Representative pictures of IHC staining of HDAC2 for tumor models. (H) TCGA database analyzed the correlation between HDAC2 and the occurrence of liver cancer. (I) TCGA database analyzed the correlation between HDAC2 and the clinicopathological stages of liver cancer. (J) TCGA database analyzed the correlation between HDAC2 and the prognosis of liver cancer. (K) Schematic diagram of LukS-PV inhibited HCC cell progression in this research.

Quantitative Proteomics Sequencing

HepG2 cells treated with LukS-PV or PBS were sonicated three times on ice using a high-intensity ultrasonic processor (Scientz, China) in lysis buffer. The supernatant was collected, and protein concentration was determined with a BCA kit according to the manufacturer's instructions. The protein solution was digested with 5 mM dithiothreitol for 30 min at 56°C and alkylated with 11 mM iodoacetamide for 15 min at room temperature in darkness. The sample was diluted by adding 100 mM tetraethyl ammonium bromide (TEAB) to urea concentration less than 2M. Finally, trypsin was added for digestion overnight. After trypsin digestion, peptide was reconstituted in 0.5 M TEAB and processed according to the manufacturer's protocol for TMT kit/iTRAQ kit. The tryptic peptides were fractionated into fractions by high pH reverse-phase high performance liquid chromatography (HPLC) using Agilent 300Extend C18 column. The peptides were subjected to nano spray ionization (NSI) source followed by

tandem mass spectrometry (MS/MS) in Q Exactive Plus (Thermo, USA) coupled online to the ultra performance liquid chromatography (UPLC). The resulting MS/MS data were processed using Maxquant search engine (v.1.5.2.8).

Xenograft Tumor Models in Nude Mice

BALB/c nude mice (4 weeks old) were purchased from Anhui Provincial Animal Center. For xenografts, 200 μL HepG2 cell suspension with approximately 5×10^6 cells was subcutaneously injected. Treatments were performed by intraperitoneal injection of LukS-PV or PBS 24 h later for 2 weeks. Tumor size was recorded every 4 days. Then 24 days after tumor inoculation, all experimental mice were sacrificed. Animal experiments were authorized by the ethics committee of University of Science and Technology of China [grant no. 2019-N(A)-144].

H&E Staining and IHC

Tumor tissue from mice was fixed with formalin; then H&E staining was performed following the manufacturer's instructions. IHC was performed using anti-Ki-67 (Proteintech, China) and anti-HDAC2 (Proteintech, China) antibodies.

Statistical Analysis

Data from two groups were analyzed using the unpaired Student's t test, and data from multiple groups were analyzed by ANOVA. *$p < 0.05$, **$p < 0.01$, or ***$p < 0.001$ was considered statistically significant.

AUTHOR CONTRIBUTIONS

Z.W. and W.Y. conceived and designed the study. F.M. and P.D. helped perform the experiments and analyzed the data. L.S. and W.C. assisted the experiments. W.Y., Y.Q., Y.M., and X.M. revised the manuscript, which was written by Z.W. All authors read and approved the final manuscript.

CONFLICTS OF INTEREST

The authors declare no competing interests.

ACKNOWLEDGMENTS

We thank Dr. James P. Mahaffey, from Liwen Bianji, Edanz Editing China, for editing the English text of a draft of this manuscript. This work was supported by the National Natural Science Foundation of China (grant 81972001) and the Fundamental Research Funds for the Central Universities (grant WK9110000007).

REFERENCES

1. Bray, F., Ferlay, J., Soerjomataram, I., Siegel, R.L., Torre, L.A., and Jemal, A. (2018). Global cancer statistics 2018: GLOBOCAN estimates of incidence and mortality worldwide for 36 cancers in 185 countries. CA Cancer J. Clin. *68*, 394–424.
2. Golabi, P., Fazel, S., Otgonsuren, M., Sayiner, M., Locklear, C.T., and Younossi, Z.M. (2017). Mortality assessment of patients with hepatocellular carcinoma according to underlying disease and treatment modalities. Medicine (Baltimore) *96*, e5904.
3. Weldon, J.E., and Pastan, I. (2011). A guide to taming a toxin–recombinant immunotoxins constructed from Pseudomonas exotoxin A for the treatment of cancer. FEBS J. *278*, 4683–4700.
4. Li, Y.M., Vallera, D.A., and Hall, W.A. (2013). Diphtheria toxin-based targeted toxin therapy for brain tumors. J. Neurooncol. *114*, 155–164.
5. Karpiński, T.M., and Adamczak, A. (2018). Anticancer Activity of Bacterial Proteins and Peptides. Pharmaceutics *10*, 54.
6. Alderson, R.F., Kreitman, R.J., Chen, T., Yeung, P., Herbst, R., Fox, J.A., and Pastan, I. (2009). CAT-8015: a second-generation pseudomonas exotoxin A-based immunotherapy targeting CD22-expressing hematologic malignancies. Clin. Cancer Res. *15*, 832–839.
7. Waldron, N.N., Kaufman, D.S., Oh, S., Inde, Z., Hexum, M.K., Ohlfest, J.R., and Vallera, D.A. (2011). Targeting tumor-initiating cancer cells with dCD133KDEL shows impressive tumor reductions in a xenotransplant model of human head and neck cancer. Mol. Cancer Ther. *10*, 1829–1838.
8. Oh, S., Todhunter, D.A., Panoskaltsis-Mortari, A., Buchsbaum, D.J., Toma, S., and Vallera, D.A. (2012). A deimmunized bispecific ligand-directed toxin that shows an impressive anti-pancreatic cancer effect in a systemic nude mouse orthotopic model. Pancreas *41*, 789–796.
9. Kerr, D.E., Wu, G.Y., Wu, C.H., and Senter, P.D. (1997). Listeriolysin O potentiates immunotoxin and bleomycin cytotoxicity. Bioconjug. Chem. *8*, 781–784.
10. Provoda, C.J., Stier, E.M., and Lee, K.D. (2003). Tumor cell killing enabled by listeriolysin O-liposome-mediated delivery of the protein toxin gelonin. J. Biol. Chem. *278*, 35102–35108.
11. Stachowiak, R., Lyzniak, M., Budziszewska, B.K., Roeske, K., Bielecki, J., Hoser, G., and Kawiak, J. (2012). Cytotoxicity of bacterial metabolic products, including listeriolysin O, on leukocyte targets. J. Biomed. Biotechnol. *2012*, 954375.
12. Sun, X.X., Zhang, S.S., Dai, C.Y., Peng, J., Pan, Q., Xu, L.F., and Ma, X.L. (2017). LukS-PV-Regulated MicroRNA-125a-3p Promotes THP-1 Macrophages Differentiation and Apoptosis by Down-Regulating NF1 and Bcl-2. Cell. Physiol. Biochem. *44*, 1093–1105.
13. Shan, W., Bu, S., Zhang, C., Zhang, S., Ding, B., Chang, W., Dai, Y., Shen, J., and Ma, X. (2015). LukS-PV, a component of Panton-Valentine leukocidin, exerts potent activity against acute myeloid leukemia in vitro and in vivo. Int. J. Biochem. Cell Biol. *61*, 20–28.
14. Zhang, P., Yu, W.W., Peng, J., Xu, L.F., Zhao, C.C., Chang, W.J., and Ma, X.L. (2019). LukS-PV induces apoptosis in acute myeloid leukemia cells mediated by C5a receptor. Cancer Med. *8*, 2474–2483.
15. Gu, J., Ding, J.Y., Lu, C.L., Lin, Z.W., Chu, Y.W., Zhao, G.Y., Guo, J., and Ge, D. (2013). Overexpression of CD88 predicts poor prognosis in non-small-cell lung cancer. Lung Cancer *81*, 259–265.
16. Hu, W.H., Hu, Z., Shen, X., Dong, L.Y., Zhou, W.Z., and Yu, X.X. (2016). C5a receptor enhances hepatocellular carcinoma cell invasiveness via activating ERK1/2-mediated epithelial-mesenchymal transition. Exp. Mol. Pathol. *100*, 101–108.
17. Chen, J., Li, G.Q., Zhang, L., Tang, M., Cao, X., Xu, G.L., and Wu, Y.Z. (2018). Complement C5a/C5aR pathway potentiates the pathogenesis of gastric cancer by down-regulating p21 expression. Cancer Lett. *412*, 30–36.
18. Xi, W., Liu, L., Wang, J., Xia, Y., Bai, Q., Xiong, Y., Qu, Y., Long, Q., Xu, J., and Guo, J. (2016). Enrichment of C5a-C5aR axis predicts poor postoperative prognosis of patients with clear cell renal cell carcinoma. Oncotarget *7*, 80925–80934.
19. Imamura, T., Yamamoto-Ibusuki, M., Sueta, A., Kubo, T., Irie, A., Kikuchi, K., Kariu, T., and Iwase, H. (2016). Influence of the C5a-C5a receptor system on breast cancer progression and patient prognosis. Breast Cancer *23*, 876–885.
20. Manzotti, G., Ciarrocchi, A., and Sancisi, V. (2019). Inhibition of BET Proteins and Histone Deacetylase (HDACs): Crossing Roads in Cancer Therapy. Cancers (Basel) *11*, 304.
21. Li, Y., Zhang, M., Dorfman, R.G., Pan, Y., Tang, D., Xu, L., Zhao, Z., Zhou, Q., Zhou, L., Wang, Y., et al. (2018). SIRT2 Promotes the Migration and Invasion of Gastric Cancer through RAS/ERK/JNK/MMP-9 Pathway by Increasing PEPCK1-Related Metabolism. Neoplasia *20*, 745–756.
22. Garmpis, N., Damaskos, C., Garmpi, A., Kalampokas, E., Kalampokas, T., Spartalis, E., Daskalopoulou, A., Valsami, S., Kontos, M., Nonni, A., et al. (2017). Histone Deacetylases as New Therapeutic Targets in Triple-negative Breast Cancer: Progress and Promises. Cancer Genomics Proteomics *14*, 299–313.

23. Weichert, W. (2009). HDAC expression and clinical prognosis in human malignancies. Cancer Lett. *280*, 168–176.

24. West, A.C., and Johnstone, R.W. (2014). New and emerging HDAC inhibitors for cancer treatment. J. Clin. Invest. *124*, 30–39.

25. Qiao, W., Liu, H., Liu, R., Liu, Q., Zhang, T., Guo, W., Li, P., and Deng, M. (2018). Prognostic and clinical significance of histone deacetylase 1 expression in breast cancer: A meta-analysis. Clin. Chim. Acta *483*, 209–215.

26. Lewis, K.A., Jordan, H.R., and Tollefsbol, T.O. (2018). Effects of SAHA and EGCG on Growth Potentiation of Triple-Negative Breast Cancer Cells. Cancers (Basel) *11*, 23.

27. Richa, S., Dey, P., Park, C., Yang, J., Son, J.Y., Park, J.H., Lee, S.H., Ahn, M.-Y., Kim, I.S., Moon, H.R., et al. (2020). A new histone deacetylase inhibitor, MHY4381, induces apoptosis via generation of reactive oxygen species in human prostate cancer cells. Biomol Ther (Seoul) *28*, 184–194.

28. He, B., Dai, L., Zhang, X., Chen, D., Wu, J., Feng, X., Zhang, Y., Xie, H., Zhou, L., Wu, J., and Zheng, S. (2018). The HDAC Inhibitor Quisinostat (JNJ-26481585) Suppresses Hepatocellular Carcinoma alone and Synergistically in Combination with Sorafenib by G0/G1 phase arrest and Apoptosis induction. Int. J. Biol. Sci. *14*, 1845–1858.

29. Shouksmith, A.E., Shah, F., Grimard, M.L., Gawel, J.M., Raouf, Y.S., Geletu, M., Berger-Becvar, A., de Araujo, E.D., Luchman, H.A., Heaton, W.L., et al. (2019). Identification and Characterization of AES-135, a Hydroxamic Acid-Based HDAC Inhibitor That Prolongs Survival in an Orthotopic Mouse Model of Pancreatic Cancer. J. Med. Chem. *62*, 2651–2665.

30. Fournier, J.F., Bhurruth-Alcor, Y., Musicki, B., Aubert, J., Aurelly, M., Bouix-Peter, C., Bouquet, K., Chantalat, L., Delorme, M., Drean, B., et al. (2018). Squaramides as novel class I and IIB histone deacetylase inhibitors for topical treatment of cutaneous t-cell lymphoma. Bioorg. Med. Chem. Lett. *28*, 2985–2992.

31. Wei, Y., Zhou, F., Lin, Z., Shi, L., Huang, A., Liu, T., Yu, D., and Wu, G. (2018). Antitumor effects of histone deacetylase inhibitor suberoylanilide hydroxamic acid in epidermal growth factor receptor-mutant non-small-cell lung cancer lines in vitro and in vivo. Anticancer Drugs *29*, 262–270.

32. Du, W., Zhang, X., and Wan, Z. (2019). miR-3691-5p promotes hepatocellular carcinoma cell migration and invasion through activating PI3K/Akt signaling by targeting PTEN. OncoTargets Ther. *12*, 4897–4906.

33. Chandrashekar, D.S., Bashel, B., Balasubramanya, S.A.H., Creighton, C.J., Ponce-Rodriguez, I., Chakravarthi, B.V.S.K., and Varambally, S. (2017). UALCAN: A Portal for Facilitating Tumor Subgroup Gene Expression and Survival Analyses. Neoplasia *19*, 649–658.

34. Ikeda, K. (2019). Recent advances in medical management of hepatocellular carcinoma. Hepatol. Res. *49*, 14–32.

35. Kao, J.H., Chen, P.J., and Chen, D.S. (2010). Recent advances in the research of hepatitis B virus-related hepatocellular carcinoma: epidemiologic and molecular biological aspects. Adv. Cancer Res. *108*, 21–72.

36. Witt, O., Deubzer, H.E., Milde, T., and Oehme, I. (2009). HDAC family: What are the cancer relevant targets? Cancer Lett. *277*, 8–21.

37. Zhang, L., Wang, G., Wang, L., Song, C., Leng, Y., Wang, X., and Kang, J. (2012). VPA inhibits breast cancer cell migration by specifically targeting HDAC2 and down-regulating Survivin. Mol. Cell. Biochem. *361*, 39–45.

38. Zhou, L., Xu, X., Liu, H., Hu, X., Zhang, W., Ye, M., and Zhu, X. (2018). Prognosis Analysis of Histone Deacetylases mRNA Expression in Ovarian Cancer Patients. J. Cancer *9*, 4547–4555.

39. Yang, Y., Zhang, J., Wu, T., Xu, X., Cao, G., Li, H., and Chen, X. (2019). Histone deacetylase 2 regulates the doxorubicin (Dox) resistance of hepatocarcinoma cells and transcription of ABCB1. Life Sci. *216*, 200–206.

40. Lee, Y.H., Seo, D., Choi, K.J., Andersen, J.B., Won, M.A., Kitade, M., Gómez-Quiroz, L.E., Judge, A.D., Marquardt, J.U., Raggi, C., et al. (2014). Antitumor effects in hepatocarcinoma of isoform-selective inhibition of HDAC2. Cancer Res. *74*, 4752–4761.

41. Papa, A., and Pandolfi, P.P. (2019). The PTEN^{-}PI3K Axis in Cancer. Biomolecules *9*, 153.

42. Zhang, H., Zhao, B., Huang, C., Meng, X.M., Bian, E.B., and Li, J. (2014). Melittin restores PTEN expression by down-regulating HDAC2 in human hepatocelluar carcinoma HepG2 cells. PLoS ONE *9*, e95520.

43. Pan, L., Lu, J., Wang, X., Han, L., Zhang, Y., Han, S., and Huang, B. (2007). Histone deacetylase inhibitor trichostatin a potentiates doxorubicin-induced apoptosis by up-regulating PTEN expression. Cancer *109*, 1676–1688.

44. Bian, E.B., Huang, C., Ma, T.T., Tao, H., Zhang, H., Cheng, C., Lv, X.W., and Li, J. (2012). DNMT1-mediated PTEN hypermethylation confers hepatic stellate cell activation and liver fibrogenesis in rats. Toxicol. Appl. Pharmacol. *264*, 13–22.

45. Conte, M., Dell'Aversana, C., Sgueglia, G., Carissimo, A., and Altucci, L. (2019). HDAC2-dependent miRNA signature in acute myeloid leukemia. FEBS Lett. *593*, 2574–2584.